

Prospects and challenges for high-pressure reverse osmosis in minimizing concentrated waste streams

A Benjamin Schantz¹, Boya Xiong², Elizabeth Dees³, David R. Moore³, Xuejing Yang^{4,5}, Manish Kumar^{1,2*}

¹Department of Chemical Engineering, ²Department of Civil and Environmental Engineering, The Pennsylvania State University, University Park, Pennsylvania 16802

³GE Global Research Center, 1 Research Circle, Niskayuna, NY 12309

⁴ Department of Civil and Environmental Engineering, University of California at Berkeley, Berkeley, CA 94720-1716, USA

⁵ National Engineering Laboratory for Industrial Wastewater Treatment, East China University of Science and Technology, Shanghai, 200237, China

*Corresponding Author

Table of Contents Entry (a 8cm*4cm figure with a caption of up to 30 words)

Abstract (50-250 words)

Reverse osmosis (RO) has become the most common process for extracting pure water from saline water, outcompeting thermal processes such as multi-effect distillation (MED) and multi-stage flash (MSF) due to its lower energy consumption and cost. RO is currently limited to treating streams with total dissolved solids (TDS) values of less than 50,000 ppm. Zero-liquid discharge (ZLD) processes using pretreatment, RO, and thermal steps can concentrate and dispose of high salinity waste brines with greater thermodynamic efficiency than a purely thermal process but such a process is not yet widely practiced. Waste streams requiring ZLD typically have total dissolved solids (TDS) as high as 300,000 ppm, and include seawater RO (SWRO) brines, flowback and produced water from unconventional shale gas development, formation water from CO₂ sequestration, and Flue Gas Desulfurization (FGD) wastewater. The TDS levels of these streams can exceed those of seawater by nearly an order of magnitude, and even to concentrate a stream with similar TDS levels to seawater, a high-pressure RO process is needed to achieve a high water recovery. In this review we consider a high-pressure RO (HPRO) process with applied pressures of 2400 – 5000 psi (compared to 800-1000 psi for SWRO) to reduce the volume of high salinity brine wastes. We discuss the challenges amplified by elevated pressure requirements and feed salinities, such as ion precipitation and scaling, biofouling, and RO module mechanical stability. We also propose solutions to address these limitations of HPRO.

Water Impact Statement

High-salinity brines from energy and water production (such as RO retentate, FGD wastewater, fracking flowback water, and formation waters from CO₂ storage aquifers) are unsuitable for surface water discharge. Limited disposal options have led researchers to study the concentration and dewatering of these brines despite the high cost and energy requirements for ZLD disposal. High-pressure RO (HPRO) could allow more energy-efficient wastewater concentration compared to existing thermal processes, and we review the challenges and possible solutions for HPRO process design, as well as options for disposing of or obtaining valuable salts and chemicals from the remaining concentrates.

1. Introduction – Opportunities for high-pressure RO (HPRO)

The management of high-salinity brines with total dissolved solids up to 350,000 ppm is a substantial challenge for industries across the Global Industrials Classification Standard (GICS) taxonomy, including energy, chemicals, healthcare, consumer products, and water utilities industries. Brines from the energy industry include oil and gas produced water¹, crude oil desalter wastewater², the spent caustic from refinery plants³, gasification or formatted wastewater from coal and consumable fuel suppliers⁴, and flue gas desulfurization processes⁵. Chemical/healthcare industry brines include waste from the processing and synthesis of chemicals, munitions⁶, drugs⁷, and some hospital wastewater⁸. Consumer product industry wastes include dairy and olive mill wastewater⁹, filature¹⁰, drying or tannery wastewater¹¹, and pulp and paper wastewater¹². Water utility brines include retentates from RO¹³⁻¹⁴, nanofiltration¹⁵, and membrane bioreactor processes¹⁶, and landfill leachates¹⁷⁻¹⁸. Several review articles have discussed high salinity waste management with a focus on common treatment techniques¹⁹, value-added mineral recovery processes²⁰, cost effective strategies²¹, and emerging contamination issues²². Here, we aim to discuss the feasibility of high-pressure reverse osmosis (HPRO) for minimizing high salinity waste streams from four representative sources that generate waste in large volumes.

These streams are SWRO brine²³, FGD wastewater⁵, and hydraulic fracturing flowback and produced waters²⁴ that are produced on a scale of millions of m³/day (**Table 1**). SWRO brines are currently discharged to the ocean, possibly disrupting the salinity and temperature of the marine environment and polluting the water with RO pretreatment chemicals²⁵. The salinity of seawater varies geographically, being relatively constant in the open ocean but higher in some regions such as the Red Sea²⁶. Similar brines are created at inland locations by desalination of brackish ground water, and these brines cannot be conveniently discharged to the ocean, so that a disposal process would be even more beneficial in these situations than for SWRO^{25, 27}. The concentrate fraction for SWRO is generally about 50-70% of the feed due to the pressure and fouling limits of a conventional SWRO process²⁸⁻³⁰. The TDS in flowback and produced water from oil and shale gas development varies greatly with the geology of the source formation, as shown in **Table 1**. The direct reuse of oil and shale gas wastewater for subsequent extraction is a common practice but is declining as the industry matures and less water is needed for developing new wells³¹. Deep well injection is another waste management method, but raises concerns about leakage and increased

seismic activity³¹. A waste brine similar to shale gas produced waters could be produced in even greater quantities if the sequestration of supercritical carbon dioxide in saline aquifers is implemented as a way to reduce global warming³². The flue gas desulfurization (FGD) process used in coal-fired power plants utilizes limestone wet scrubbing to control SO_x emissions, generating a CaSO₄-rich wastewater⁵ whose composition varies depending on the composition of the coal and limestone. FGD wastewater is treated by chemical precipitation, filtration, and solids dewatering before release, so that heavy metal (Se) removal is incomplete⁵. Because of these environmental risks associated with waste brine disposal, alternative disposal methods have become a growing field of research.

ZLD processes have been proposed as a way to better dispose of such brines, and to produce valuable salts and chemicals from the remaining solids to help offset the disposal costs^{20, 25, 27, 33-36}. However, ZLD can come with unintended consequences: a review of the expenses and environmental impacts of FGD wastewater disposal by a ZLD process using chemical treatment, membrane vapor compression (MVC), and thermal crystallization showed that ZLD would cause more environmental damage than the current disposal process³⁷. This environmental damage comprises the air pollution and climate change that result from using the current mix of power plants to meet the high energy demands of MVC and crystallization³⁷. Consequently, reducing the energy usage in brine concentration would make ZLD much more environmentally friendly^{28, 35}. A part of the thermal ZLD processes with substantial room for energy efficiency improvement is the MVC step: its thermodynamic efficiency is only 5-10%³⁸⁻³⁹, with the lost thermal energy deriving from the temperature difference between the feed and heating fluid⁴⁰. Reverse osmosis and Forward Osmosis (FO) are two more energy-efficient separation processes that might be used to replace MVC. In RO, the feed solution is hydraulically pressurized and then separated into fresh water and concentrated brine using a water-permeable and salt-rejecting membrane²⁹⁻³⁰, where as in FO, a concentrated draw solution and a water-permeable, salt-rejecting membrane are used to remove water from the feed and the draw solution is re-concentrated (regenerated) using RO or a thermal process⁴¹. Of these two methods, RO is more efficient because the draw solute regeneration step in FO requires a greater change in osmotic pressure and thus a greater minimum energy input than the alternative RO process^{31, 41-42}. In absolute (thermodynamic) terms, SWRO processes can achieve at least 50% energy efficiency at the optimum operating condition of 50% recovery, and continue to increase in energy efficiency; they already closely approach the thermodynamic limit due to improvements in membrane technology³⁰. However, RO membranes and processes have not been designed for these high-salinity conditions (challenges include mechanical stability at high pressure, and minimizing RO membrane fouling, which is less reversible than FO membrane fouling due to compaction under pressure), so that MVC and FO are currently the methods used to separate these brines^{37, 41}.

Concentrated waste brines have a higher osmotic pressure than seawater, and thus require a higher applied pressure to concentrate, although the energy efficiency of HPRO and SWRO processes should be similar if RO modules capable of withstanding these pressures are designed. **Figure 1A** shows the osmotic pressure as a function of feed concentration, and the typical concentration ranges of the four concentrated waste streams discussed in this review are presented. Typical SWRO operates at 800-1000 psi²⁹, where as for HPRO we consider pressures up to 5000

psi, making the assumption that this does not exceed the burst pressure of the membrane. The minimum energy needed to remove pure water from a salt solution (independent of the process used) can be calculated by integrating the osmotic pressure with respect to the volume of water removed using equation S8⁴³, and the results are summarized in **Figure 1B**. This minimum energy is known as the thermodynamic limit³⁰. SWRO has a thermodynamic limit of 1-1.5 kWh/m³, where as an HPRO process would require a minimum of 3-9 kWh/m³ for a 100-200 g/L feed. The thermodynamic efficiency is the quotient of this minimum energy and the energy actually used for the separation^{30,40}. In addition to the minimum energy, a realistic RO process requires an applied pressure higher than osmotic pressure to separate pure water from brine on a finite time scale (the difference between the applied and osmotic pressures is called the overpressure)³⁰. Also, the applied pressure in a real RO module is less than or equal to the inlet pressure rather than continuously increasing with the increasing feed-side osmotic pressure (as it would in a reversible process)⁴⁴. Thus, the energy efficiency of a single-stage (or multi-stage) RO process would be less than 100% even without an energy cost due to pressure drop within the module or pre/post-treatment. **Figure 1C** shows that for an idealized single-stage RO process with these assumptions, the energy efficiency is between 60 and 80% for a range of concentrations and water recoveries pertinent to SWRO and HPRO. **Table 1** summarizes the optimum separation performance (energy use and recovery) of an ideal HPRO process (2500-5000 psi) to reduce the volume of four common brines generated during energy and water production. The calculations used to produce these data are discussed in more detail in Supporting Information. These brines can be significantly concentrated by HPRO at 5,000 psi, and some of the less concentrated brines (with lower osmotic pressure) can also be concentrated with an applied pressure of 2,500 psi. For each concentrated waste brine, the thermodynamic limit is calculated for these two applied pressures. Thus, HPRO could theoretically achieve an energy efficiency of about 60-80% compared to 5-10% for a MVC process, providing a more energy-efficient alternative for high salinity brine disposal.

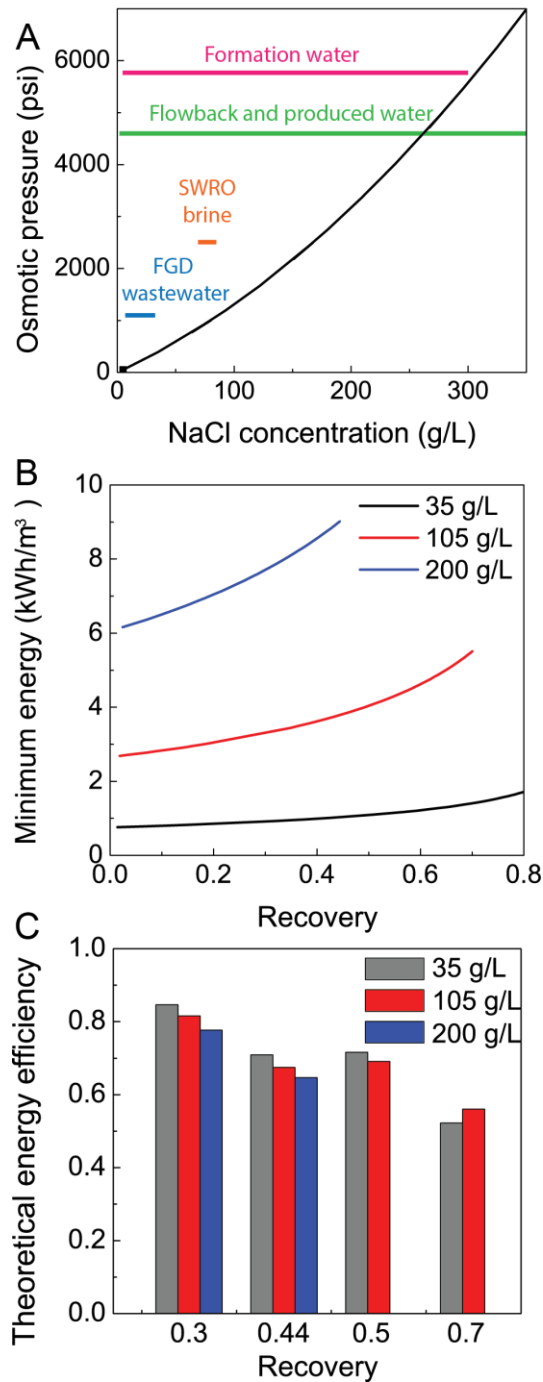


Figure 1. (A) Osmotic pressure and salt concentration range of the four different types of feed brines discussed in this review. (B) Theoretical minimum energy for desalination as a function of percent recovery for three different feed salinities. Each curve ends at a recovery corresponding to a retentate saturated with NaCl; at higher recoveries, detrimental salt precipitation would occur. (C) Maximum energy efficiency of a single stage RO process as a function of recovery is similar among feeds with different concentrations. Energy efficiency is calculated as the ratio of the thermodynamic minimum to the single-stage minimum energy. The maximum recovery for a feed concentration of 200 g/L is 44% because the retentate is a saturated NaCl solution at this recovery.

Table 1: Properties of high-pressure RO feed waters. These ideal values are calculated assuming a lack of fouling and concentration polarization, and that all divalent cations (which cause scaling²⁹) are removed during pretreatment. In addition, the osmotic pressure is calculated using a simple empirical model for NaCl-water solutions⁴⁵.

	SWRO brine ²³ (50% recovery)	Flowback water ²⁴	Formation water ³²	FGD wastewater ⁵
TDS [mg/L]	~72,000 – 82,000	~30,000 – 130,000	~5,000 – 300,000	~5,000 – 50,000
Volume Produced* [millions of m³/day]	60 worldwide	9 in the U.S.	Potential for 130 - 150 worldwide	2.2 (worldwide) 0.14 (U.S.)
$\Delta\pi$ total [psi]	~1900 – 2200	~750 – 3100	~50 – 5600	~90 - 1000
$\Delta\pi$ from monovalent salts [psi]	~1700 – 2000	~640 – 2800	~50 – 4900	~35 - 700
Major ions [symbol, mg/L]	Cl ⁻ (40,000), Na ⁺ (22,000), Mg ²⁺ (2600), K ⁺ (800)	Na ⁺ (13,000), Cl ⁻ (12,000), Ca ²⁺ (3600), HCO ₃ ⁻ (1200), Sr ²⁺ (1100), CO ₃ ²⁻ (800), Br ⁻ (300), K ⁺ (300), CO ₂ (300), Ba ²⁺ (200), Mg ²⁺ (200), SO ₄ ²⁻ (200)	Cl ⁻ , Na ⁺ (~10,000 each), Ca ²⁺ , Br ⁻ , HCO ₃ ⁻ , SO ₄ ²⁻ , NO ₃ ⁻ , Mg ²⁺ , K ⁺ (100-1000 each)	Cl ⁻ (1000-28,000), SO ₄ ²⁻ (1500-8000), Mg ²⁺ (1100-5000), Na ⁺ (700-5000), Ca ²⁺ (750-4000), SiO ₂ (70)
Max recovery** (2500 psi)	16 to 26%	0 to 67%	0 to 97%	65 to 98%
Min $\Delta G_{\text{separation}}$ at 2500 psi [kWh/m³ permeate]	3.9 to 4.3	2.3 to 4.8	0.4 to 4.8	0.3 to 2.4
Max recovery** (5000 psi)	49 to 55%	35 to 80%	2 to 98%	79 to 99%
Min $\Delta G_{\text{separation}}$ at 5000 psi [kWh/m³ permeate]	5.4 to 5.9	3.0 to 7.0	0.4 to 9.4	0.4 to 3.1

*Methods for calculating the volume produced are given in Supporting Information.

**The minimum retentate fraction corresponds to an ideal separation process, in which multivalent ions are removed during pretreatment; water permeation proceeds to equilibrium; and concentration polarization, feed-side pressure drop, and membrane fouling are absent.

Despite operating closer to the minimum energy requirements than a thermal process, RO is mechanically limited by the range of applied pressures. Conventional SWRO is limited to pressures of approximately 1,200 psi due to the strength limits of membrane materials and spiral-wound module⁴⁴. Treatment of high salinity waste brines would benefit from a higher applied pressure (we consider 2,500-5000 psi, although we calculate that a pressure as high as 7,300 psi could be used to bring these brines to the saturation point^{43, 46}). Following concentration by HPRO, the remaining water would be removed by a thermal process such as MVC or a crystallizer (**Figure 2**). RO processes with applied pressure as high as 3,000 psi have been conducted since the 1980's to concentrate landfill leachates using disc-tube RO modules made from stainless steel and high-performance plastics^{28, 47-49}. Such modules can produce similar permeate flow rates and require costs similar as those of spiral-wound modules, presenting an attractive option for brine concentration. This review will discuss the pretreatment requirements for such a process, the concentration polarization and fouling challenges that would reduce module performance, and how we might design efficient RO modules for high-pressure operation.

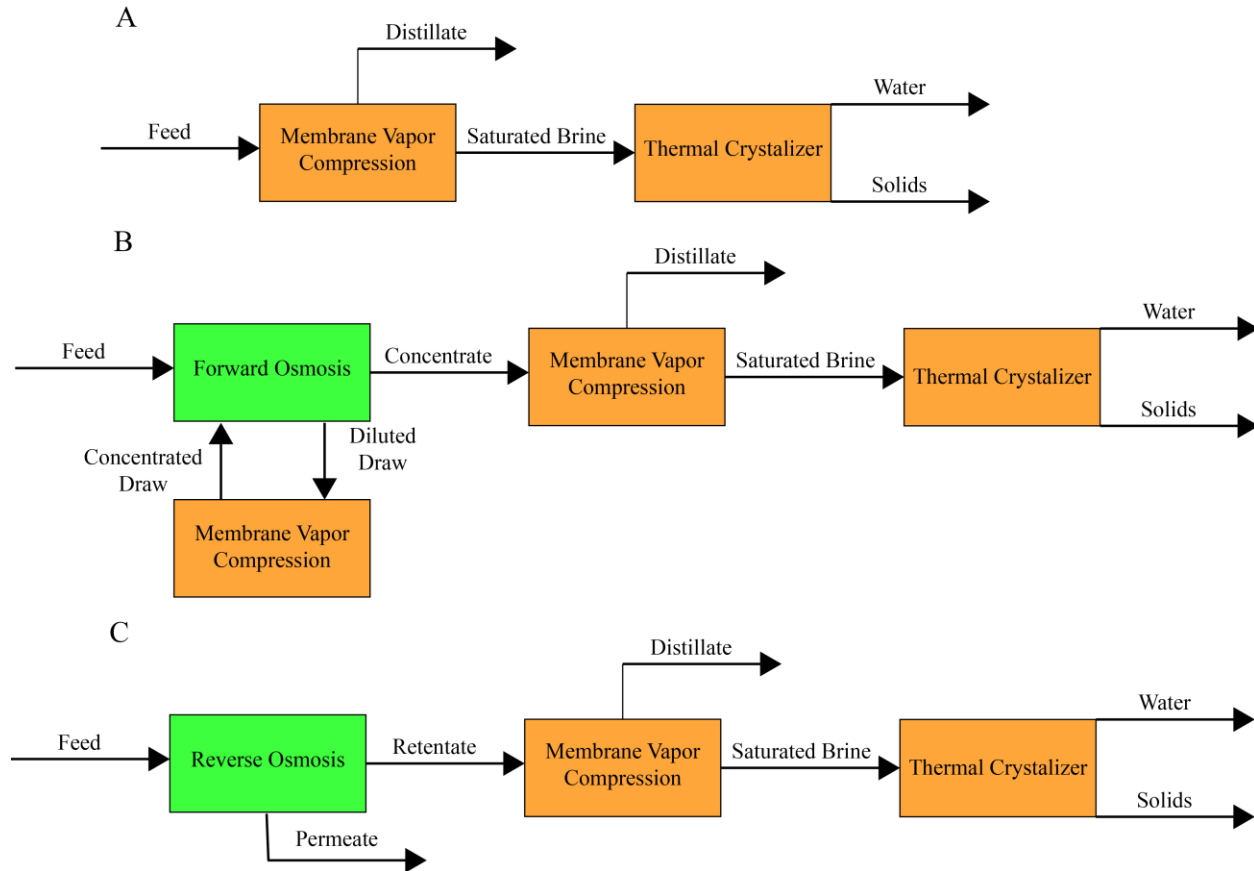


Figure 2: Process-flow diagram for a ZLD process using (a) thermal methods, (b) FO, and (c) HPRO. Note that in cases b and c, a thermal process is still required to remove the remaining water from the feed following the membrane process. Thermal processes (less efficient) are shown in yellow, while membrane processes (more efficient) are shown in green. By removing some water from the feed with a membrane process, we can increase the overall ZLD efficiency.

2. Challenges for high-pressure RO

2.1 Concentration polarization

Concentration polarization (CP) is a familiar phenomenon in reverse osmosis, in which the selective permeation of water through the membrane leaves a layer of high salt concentration near the membrane surface. The thickness and salt concentration profile of this layer depend on the balance between convection towards the membrane and back-diffusion of salt⁵⁰. Numerous models have been proposed to quantify CP. Because the Film Theory model is simple, analytically solvable, and predicts experimental results as well as the more rigorous numerical methods⁵¹⁻⁵², it is preferred by many process engineers⁵², and we use it to better understand how concentration polarization might be different at higher recoveries and salt concentrations. This model can be derived by solving the salt mass balance in the high-salt boundary layer near the membrane surface to obtain the ratio of bulk and surface salt concentrations C_m/C_b . This ratio is also known as the concentration polarization (CP) modulus β , and is given by:

$$\beta = e^{J_w/k} \quad (1)$$

Where J_w is the permeate water flux [m/s] and k is the mass transfer coefficient describing salt diffusion [m/s]. The mass transfer coefficient can be calculated as the ratio of the boundary layer thickness δ [m] to the salt diffusion coefficient D [m²/s]⁵², and related to the Reynolds and Schmidt numbers Re and Sc via an empirical correlation⁵¹:

$$k = \frac{D}{\delta} = 0.023 \frac{D}{d_H} Re^{0.83} Sc^{0.33} = 0.023 \frac{D}{2h} Re^{0.83} Sc^{0.33} \quad (2)$$

Where d_H is the hydraulic diameter and h is the feed channel height [m]. The relationship $d_H = 2h$ is true for a spiral-wound module because the channel cross-section is a narrow slit (width $w \gg h$), leading to a hydraulic diameter of:

$$d_H = \frac{4(\text{flow cross section})}{\text{wetted perimeter}} = \frac{4wh}{2w+2h} \approx 2h \quad (3)$$

Using the definition of recovery in terms of the permeate and feed flow rates, as well as module geometry, we can re-write the permeate flux in terms of recovery and geometric parameters:

$$r = \frac{Q_P}{Q_f} = \frac{LwJ_w}{whv} = J_w \frac{L}{vh} \quad (4)$$

$$\beta = e^{J_w/k} = e^{rvh/Lk} \quad (5)$$

Where r is the water recovery in the permeate, v is the feed velocity, L is the length of the membrane, and Q_P and Q_f are the permeate and feed flow rates. For a fixed module design, v , J_w , and r are the adjustable parameters. For a constant value of J_w , increasing v will increase the Reynolds Number and thus increase the mass transfer coefficient and decrease concentration polarization. This requires operating at a lower recovery ratio, using a longer train of membrane modules (higher L), or recycling some of the retentate, the second two solutions being common in SWRO. In addition, the use of feed spacers to promote mixing will reduce concentration polarization at constant v and J_w ⁴⁴. For a typical RO design, concentration polarization will increase only moderately ($\beta < 2$) at the high recoveries used in a ZLD process, as shown in **Figure 3**.

It is also worth mentioning that although the Film Theory model for the CP modulus has no explicit dependence on pressure or salt concentration, high salt concentrations will influence CP through changes in salt activity and diffusivity. At sufficiently high salt concentrations, the chemical potential of the salt in solution increases quadratically rather than linearly with salt concentration, so that the salt back-diffusion (which is proportional to the activity gradient) should increase compared to the Film Theory Model's prediction^{29, 53-54}. The result will be lower concentration polarization than predicted by the Film Theory model, occurring at salt concentrations \geq about 120-180 g/L⁵³⁻⁵⁴. Our assumption of constant salt diffusivity is also not precisely correct but is a common design approximation. NaCl diffusivity remains approximately constant (1.47 to 1.60 x10⁻⁹ m²/s, with a slight increase as NaCl concentration increases from approximately 29 g/L to 230 g/L)⁴⁶. These small changes in diffusivity modify the CP modulus by 0.1 or less under the conditions studied, and the increased diffusivity slightly reduces

concentration polarization (**Figure 3**). However, if the salt concentration exceeds about 320 g/L, the diffusivity declines rapidly and would eventually reach zero at the spinodal limit of 360 g/L⁴⁶, leading to a significant increase in concentration polarization.

Finally, the film thickness δ will increase in the feed flow direction rather than being constant (as is commonly assumed), causing a decrease in the CP mass transfer coefficient k , but the equation for this increase will depend on the flow profile⁵². Thus, concentration polarization will be the most severe in the last module of the RO train, and care should be taken to prevent concentrations exceeding 320g/L NaCl in any part of the process. We also note that at the higher recoveries used for HPRO ($r > 50\%$), the CP modulus will be noticeably higher than for SWRO: 1.07- 1.14 at 50% recovery (commonly used for SWRO), 1.1-1.2 at 70% recovery, and 1.15-1.3 at 99% recovery.

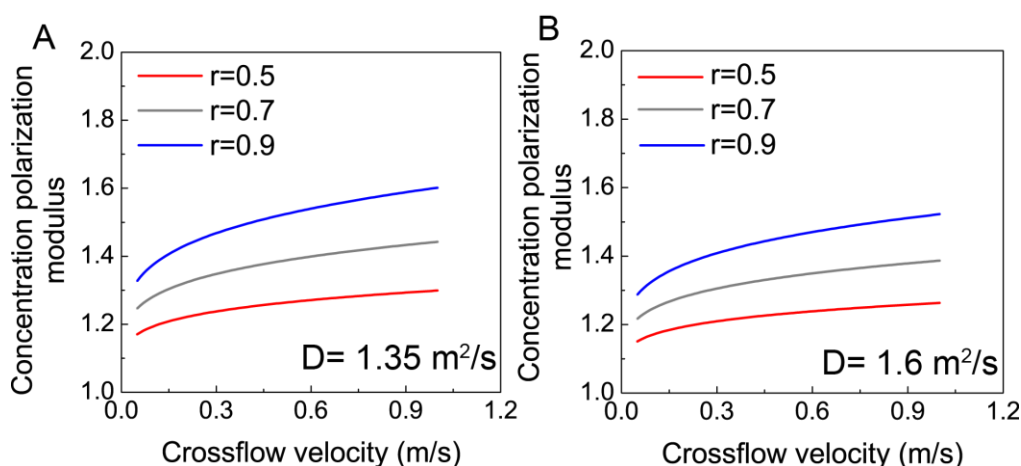


Figure 3: Concentration polarization modulus increases with crossflow velocity and recovery (r), provided that NaCl concentration remains below about 320 g/L. (A) $D= 1.35 \text{ m}^2/\text{s}$, (B) $D= 1.6 \text{ m}^2/\text{s}$. The following values were used in the film theory model: $\rho = 1000 \text{ kg}/\text{m}^3$, $\mu = 0.001 \text{ kg}/\text{m}\cdot\text{s}$, $h = 0.00025 \text{ m}$, and $L = 10 \text{ m}$. These results are approximately independent of salt concentration assuming that salt activity is linearly proportional to salt concentration (thus, the CP modulus may be lower than predicted at salt concentrations $\geq 120\text{-}180 \text{ g}/\text{L}$).

2.2 Scaling

Scaling due to salt precipitation is a frequently-occurring issue in conventional RO, and will be increased for high-pressure systems with highly concentrated retentates and a diverse mix of salts in the feed. To prevent scaling, about 99% of the divalent cations must be removed during pretreatment²⁷, and quicklime (CaO) and soda ash (Na_2CO_3) are the compounds used to remove carbonate and noncarbonate hardness respectively^{51, 55}. CaO precipitates CO_2 , HCO_3^- , Mg^{2+} , and Ca^{2+} as carbonates and hydroxides at pH 9.3-10.5⁵¹ (shown in equations S9-S12). Soda ash (Na_2CO_3) removes the remaining divalent cations⁵¹ (equation S13). Next, we compare the CaCO_3 -equivalent concentrations of Ca^{2+} , Mg^{2+} , and HCO_3^- (calculated using equation S14) to determine the amount of calcium and magnesium hardness that will precipitate via reactions involving bicarbonate salts. The calcium precipitates preferentially, followed by magnesium and other cations if sufficient bicarbonate is present. We then calculate the quicklime required to precipitate

the carbonate hardness (CO_2 + bicarbonate salt reactions) and the soda ash required to precipitate the noncarbonate hardness (the remaining salts) using equations S15 and S16. Chemical reactions for this process are described further in supporting information.

Barium, magnesium, and calcium can also be removed by a fluidized weak cation exchange process²⁷, although softening by chemical addition is more common for Ca^{2+} , Sr^{2+} , and Mg^{2+} . BaCO_3 and $\text{Ba}(\text{OH})_2$ are both relatively water-soluble, so that Ba^{2+} cannot be removed with soda ash or quicklime. Fortunately, however, BaSO_4 has a relatively low solubility limit (2-3mg/L)⁵⁶, so that the ~200mg/L Ba^{2+} and ~200mg/L SO_4^{2-} in flowback water should precipitate. If the flowback water from a well is rich in Ba^{2+} but not SO_4^{2-} , Na_2SO_4 can be used as a precipitant⁵⁶. For feeds with high silica content, additional pretreatment will be needed to prevent irreversible silica deposition on the membrane, which occurs at ~120 mg/L²⁹. Methods for silica removal include electrocoagulation with aluminum anodes (removes ~80% of the silica⁵⁷) and coprecipitation with lime and soda ash (68% removed⁵⁸). These processes are necessary to prevent formation of impermeable silica layers.

Based on current quicklime and soda ash prices, we calculate the costs for chemical softening for HPRO feeds (shown in **Table 2**). These costs (between \$0.84 and \$4.22/m³) are substantial compared to that of SWRO desalination 0.58/m³ for a modern plant⁵⁹), although they are comparable to costs for small-scale (250-1000 m³/day) SWRO installations (\$1.25-\$4/m³)⁶⁰. Pretreatment chemical costs are also only a fraction of the roughly \$25/m³ cost of oil and gas produced water disposal by well injection (which includes transportation, capital costs, and O&M)⁶¹. Thus, depending on the other separation costs, high-pressure RO may be an economical method for treating fracking flowback water and formation water, or at minimum a more environmentally friendly method that could also provide irrigation-quality water⁶¹.

Table 2: Pretreatment requirements for HPRO feeds. Typical feed compositions and softening chemical costs of \$65/ton for quicklime and \$210/ton for soda ash were used in these calculations.

	SWRO brine (50% recovery)	Fracking flowback water	Formation water	FGD water
Ions removed [name, mg/L]	Mg^{2+} (1300)	Ca^{2+} (3600), HCO_3^- (1200), Sr^{2+} (1100), CO_2 (300), Mg^{2+} (200), Ba^{2+} (200), SO_4^{2-} (200)	Ca^{2+} , HCO_3^- , Mg^{2+} (assume a high concentration of 1000 each)	Ca^{2+} (3000), Mg^{2+} (2400) (using average concentrations)
Carbonate hardness [mg/L as CaCO_3]	0	~1970 from Ca^{2+} and HCO_3^- , ~1820 from CO_2	~1640 from Ca^{2+} and HCO_3^-	0
Non-carbonate hardness [mg/L as CaCO_3]	~3250	~820 from Mg^{2+} , ~7030 from remaining Ca^{2+}	~4090 from Mg^{2+} , ~860 from remaining Ca^{2+}	~17,000
CaO required [mg/L]	~1820	~3280	~3210	5510
Na_2CO_3 required [mg/L]	~3450	~8320	~5250	~18,000
Treatment cost [\$/m ³]	~0.84	~2.24	~1.31	~4.22

2.3 Biofouling

Biofouling is also likely to be a substantial challenge for high-pressure RO. Biofilms form on both membranes and spacers⁶²⁻⁶³ and the cells and extracellular polymeric substances (EPS) form cakes that enhance concentration polarization and reduce flux⁶². Pressures of 220,000-2,200,000 psi are needed to kill most bacteria via protein denaturation and/or lipid membrane phase changes upon compression, with the required pressure varying between bacterial species⁶⁴. The pressure required to kill bacterial also increases with the salt concentration of the solution that the bacteria grow in⁶⁴. However, lower pressures than this can kill or slow the growth of some bacterial species. ZoBell *et al* found that most terrestrial bacteria grow more slowly at 4500 psi and are not viable at 9000 psi⁶⁵. In comparison, marine bacteria are more variable, and some can grow as quickly at 9000 psi as at atmospheric pressure⁶⁵. In addition, while biofilm formation is known to depend on hydrophobic and electrostatic interactions with the membrane surface, adsorption of macromolecules to membrane surfaces, membrane surface roughness, hydrodynamics, pH, nutrients, divalent cations concentration, and bacterial flagellar mobility⁶², there is no previous discussion of the effect of pressure on biofilm growth on membrane surfaces. Two types of bacteria known to form biofilms in RO modules are *E. coli* and Mycobacterium strain BT2-4⁶². *E. coli* in suspension grows as quickly at 4500 psi as at atmospheric pressure and more slowly at up to 7500 psi. Although Mycobacterium strain BT2-4 has not been studied at high pressure, two Mycobacterium species (*phlei* and *smegmatis*) are known to grow at a reduced rate at 4500-6000 psi⁶⁵. To the best of our knowledge, the highest pressure at which biofilm formation has been studied is 1300 psi (such a biofilm is shown in **Figure 4**)⁶⁶. These dense biofilms were as effective as those grew under ambient conditions at clogging a porous substrate. Likely, biofilm formation will persist at the pressures of HPRO (2500-5000 psi).

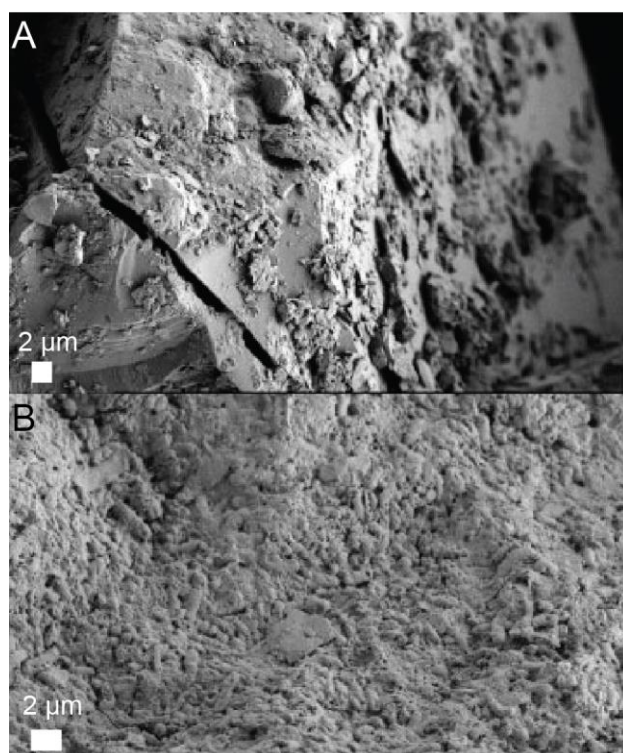


Figure 4: (A) A clean sandstone substrate and (B) the surface after one month of biofilm growth at 1300 psi. Reproduced with permission from Mitchell, et al. ⁶⁶

Once formed, biofilms are extremely resilient and cannot be removed through chemical cleaning (including with supercritical CO₂⁶⁶), lack of nutrients⁶⁶, or quorum quenching agents such as vanillin⁶⁷. Thus the focus of research is to prevent biofilm formation. Incorporation of colloidal silver particles with antimicrobial effects into the membrane or spacers has been shown to delay biofouling⁶⁸. Re-design of feed spacers to eliminate biofilm nucleation sites such as crossed support beams⁶³ also reduces biofilm formation, and biofilm nucleation at such sites is shown in **Figure 5**. The feed spacer is necessary in current module designs to create local vorticity and reduce concentration polarization⁴⁴. However, one patent describes a method for adding ridges and baffles to a spiral-wound membrane to create local vorticity without a feed spacer⁶⁹. Finally, quorum quenching agents have been shown to suppress biofilm formation, and include furanones (effective and widely studied but toxic), vanillin (nontoxic and reduced biofilm coverage by 97% after 1 week), salicylic acid, urosolic acid, cinnamaldehyde, garlic extract, and cranberry extract⁶⁷. Periodic cleaning, including sterilization with formaldehyde, peroxide, or peracetic acid solution and bacteria removal using alkalis and surfactants can increase the membrane lifetime but also degrades the membrane over time²⁹, so that proper biofilm prevention is essential.

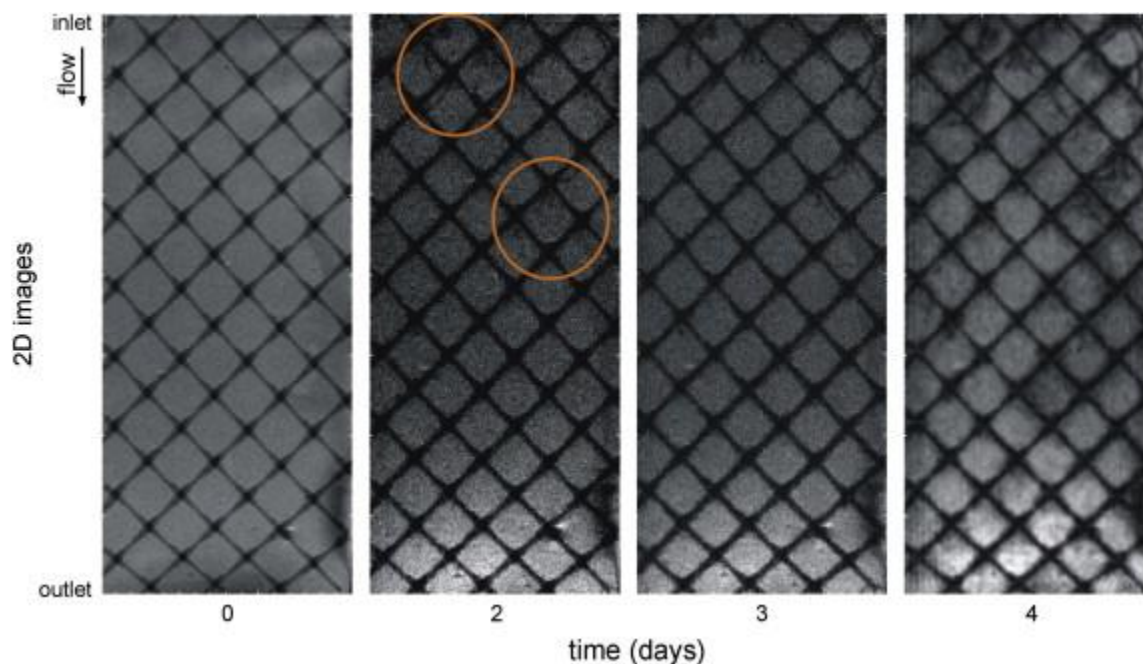


Figure 5: The intersections of the feed spacer supports in spiral-wound RO modules serve as nucleation sites for biofilm formation. Thus, improved feed spacers (or modules that can function without them) are one method for reducing biofilm growth. Reproduced with permission from Vrouwenvelder, et al. ⁶³.

2.4 Mechanical Stability at high pressure

One final challenge for high-pressure RO is the mechanical stability of RO modules at high pressure. Current spiral-wound and hollow-fiber modules are limited to about 1200 psi⁴⁴ due to the materials used in their construction. However, designing high-pressure modules is certainly possible; the disc-tube modules commonly used for concentrating landfill leachates prior to drying

via a thermal process operate around 1800-3000 psi^{28, 47, 70}. Such a module is shown schematically in **Figure 6**; in this design the feed flows around a series of membrane-coated hydraulic discs, and the permeate enters these discs before flowing to a central connecting tube. One example of a disc-tube module design is the Pall Corporation's DTGE-HHP, which operates at a pressure of 2350 psi and feed flow rate of 29 m³/day with permeate fraction 0.9-0.95, and has a 0.2 m internal diameter and 1.4 m length⁴⁹, making it similar in size and throughput to spiral-wound RO modules (typically 34-38 m³/day²⁹). Materials used include a fiber-reinforced plastic pressure tube, a polyoxymethylene water-tight flange, a stainless steel pressure flange, and an acrylonitrile butadiene styrene spacing disc⁴⁹. Benefits of disc-tube modules also include easy cleaning and turbulent flow⁴⁹, both important to operation under high-fouling conditions, although they are also more expensive than spiral-wound modules (the DTGE-HHP module costs about \$1400-\$1600, and Pall's other disc-tube modules cost about the same compared to a typical cost of about \$700 for a GE Water spiral-wound module). Pressure limits for a broader variety of disc-tube RO modules are given in **Table 3**, which shows that values of almost 3000 psi have been achieved on the pilot scale.

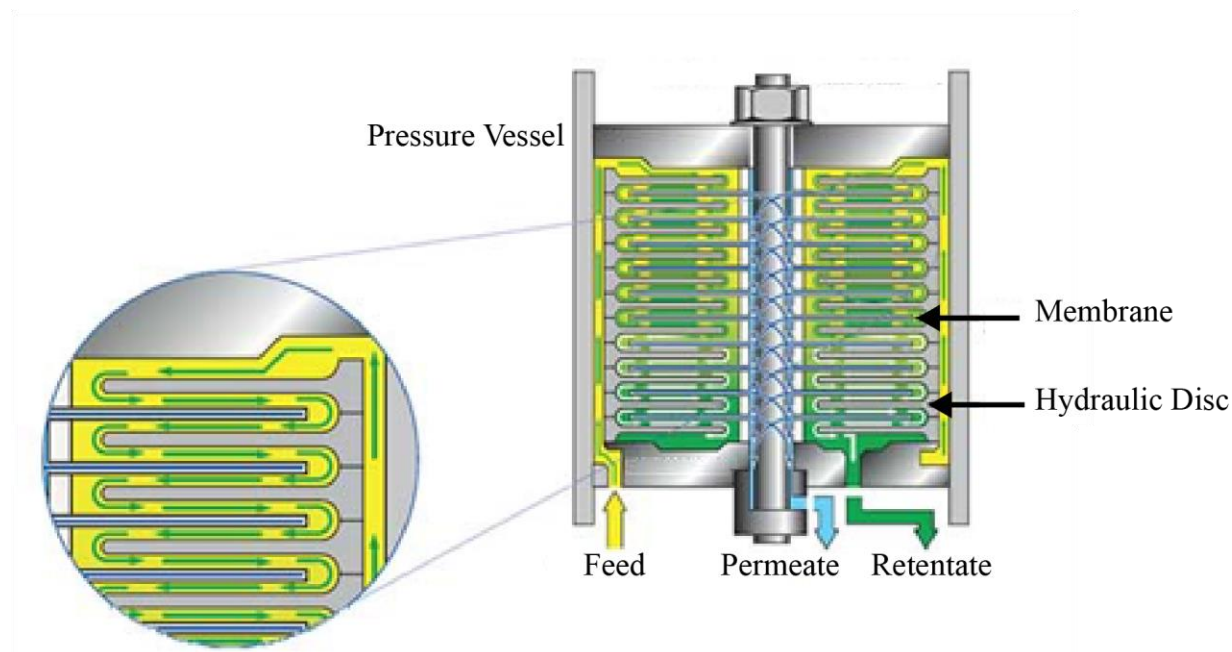


Figure 6: Schematic of a disc-tube RO module, courtesy of Pall Corporation. Copyright Pall Corporation 2018⁴⁹.

Table 3: Specifications for a variety of commercially available disc-tube RO modules, as well as one custom module used in a pilot-scale study of higher-pressure operation.

Manufacturer	Module Name	Maximum Operating Pressure [psi]
ROTREAT ⁷¹	RCDT Module 2.0 M-High Pressure	2350
Pall Corporation ⁴⁹	DTGE-HHP	2350
Rising Sun Membrane Technology ⁷²	Super High Pressure SG-DTRO-2	1760
Rochem Separation Systems ⁷³	DTM	1760
Pilot-scale custom design ⁷⁰		2940

However, most RO modules are spiral-wound, and high-pressure modules of this type might be designed given improved materials and a proper understanding of the failure mechanisms at high pressures. **Figure 7** shows such a module schematically; water enters the feed flow channel (which contains a spacer), and then permeates across the membranes and into the space within each membrane leaf. From there, the permeate flows towards a central collection tube from which it exits the module. To the best of our knowledge, the failure mechanisms of spiral-wound modules are not discussed in detail in the publically available literature. However, collapse of the permeate collection tube and failure of the membrane leaves at the collection tube junction are two common failure mechanisms known in industry (David Moore, personal communication). Two other failure mechanisms discussed in literature are telescoping (mitigated using an anti-telescoping end-cap⁴⁴) and module rupture due to pressure gradients during startup (eliminated by adding vents to the anti-telescoping device (ATD) to allow water to fill the module quickly and uniformly⁷⁴). Better understanding of these failure mechanisms and the design improvements needed to counteract them would be a good direction for future research.

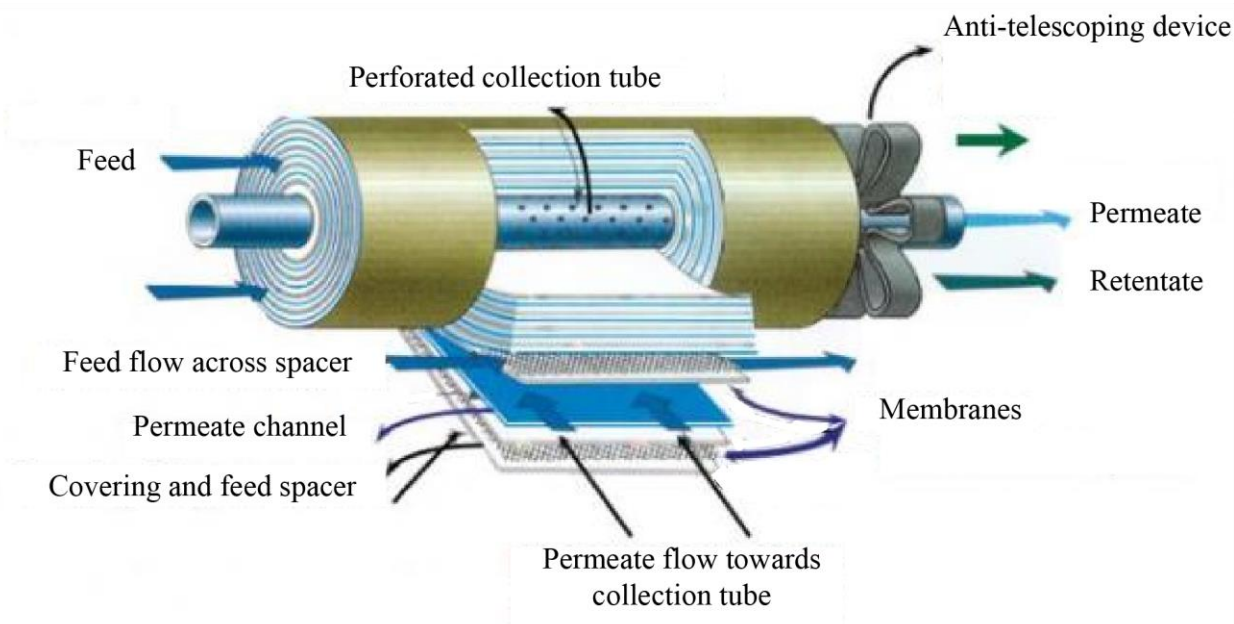


Figure 7: Schematic of a spiral-wound RO module, modified with permission from Buecker⁷⁵. A single permeate carrier and the membranes separating it from the feed solution constitute one membrane leaf.

Regardless of module design, one problem that will be more important to mitigate at high pressure is membrane compaction. When a pressure difference is applied across a membrane, voids within the membrane shrink or collapse, and this compaction reduces the membrane permeability⁷⁶⁻⁷⁸. The extent of compaction reaches a steady state after initially increasing with time⁷⁹, and is greater for a higher applied pressure difference^{78, 80}. To mitigate this problem, a number of groups have created composite membranes that incorporate mechanically strong nanoparticles^{79, 81-82}, which minimize the measured decrease in membrane thickness and loss of water flux, particularly if they are incorporated into the membrane's thin selective surface layer, which plays a key role in

determining water permeability and the effects of compaction⁸⁰⁻⁸¹. Another method for reducing membrane compaction would be to use a mechanically stronger membrane material. The limited literature available suggests that the burst pressure of a polyamide tube is about 2,500-4,600 psi at room temperature⁸³ although the burst pressure for specific aromatic polyamide composite membranes is not reported. The modulus for the selective surface layer of current polyamide RO membranes is about 1 GPa⁸⁴, so materials for HPRO membrane surface layers should have a modulus no less than this value.

3. Enabling Technologies for high-pressure RO

3.1 Module design improvements

Most current RO facilities use a standard module configuration with 0.2 m width and 1 m length that is well-studied and well-supported, researchers continue to optimize spiral-wound RO module designs. To maximize the water recovery in the permeate, it is important to minimize the feed-side pressure drop per unit length (and thus maintain the driving force for water permeation across the membrane)^{29, 44}. Otherwise, the water flux in the later part of the module will be reduced, reducing the module efficiency overall, a particularly important concern for brine disposal applications, in which our goal is to remove as much water as possible from a feed with high osmotic pressure. Feed spacer design is an important consideration in minimizing feed-side pressure drop: pressure drop per unit length increases with increasing feed spacer support density⁴⁴. A dense feed spacer network also creates more available nucleation sites for biofouling⁶³. On the other hand, the benefit of a dense feed-spacer network is that the spacer can prevent feed channel compaction during module manufacturing, and reduce concentration polarization (which is also a more serious problem at high recoveries) by creating local vorticity⁴⁴. Membranes with built-in baffles on their surfaces to create local vorticity without a feed spacer may provide a way to avoid this trade-off⁶⁹. Another method for reducing feed-side pressure drop is to reduce the length of the RO train by using wider modules with greater membrane area and permeate production per ^{44, 85}. Based on these considerations, a consortium of manufacturers decided to produce modules with a diameter of 0.4 m as a second standard size. These modules have been installed in 24 RO facilities worldwide, and their benefits include reduced floor space and piping required compared to 0.2 m modules, thereby reducing capital costs^{44, 59}.

A number of additional changes have been suggested for improving spiral-wound module design. In a spiral-wound module, the permeate is collected in membrane leaves and flows towards a central permeate tube, from which it exits the module (Figure 5). Spiral-wound leaves have a permeate-side pressure drop per unit length that depends on leaf width w , permeate spacer friction coefficient k , and local flow rate q ⁴⁴:

$$\frac{dP}{dx} = -k \frac{q}{w}$$

Here, x is the permeate flow direction (towards the central permeate tube). The permeate flow within the leaf increases and pressure decreases moving towards the central permeate tube, so that

more water passes through the membrane closer to the permeate tube. This uneven use of the membrane area leads to premature fouling of the over-used area while the membrane far from the collection tube is underused⁴⁴. This problem of uneven transmembrane flux is mitigated by reducing leaf length: shorter leaves minimize the flux difference along the length of the leaflet and thus improve membrane efficiency, as shown in **Figure 8**. Consequently, we recommend using a larger number of leaves (rather than an equal number of longer leaves) when module diameter increases⁴⁴.

Another concern for high-pressure applications is the need for thicker pressure vessels to accommodate higher operating pressures and wider RO modules. The specific module improvements required for high-pressure operation at 2500-5000 psi have not been previously discussed and the additional capital cost cannot be quantified at present. However, this additional capital cost could be counteracted by a wider diameter module design that reduces piping and the number of RO trains. The Sorek plant (completed near Tel Aviv in 2013) was the first large-scale conventional SWRO facility to use 0.4 m wide modules. The use of these modules in combination with high-efficiency pumps and energy recovery devices results in a lower water production cost than at any previous SWRO facility⁵⁹.

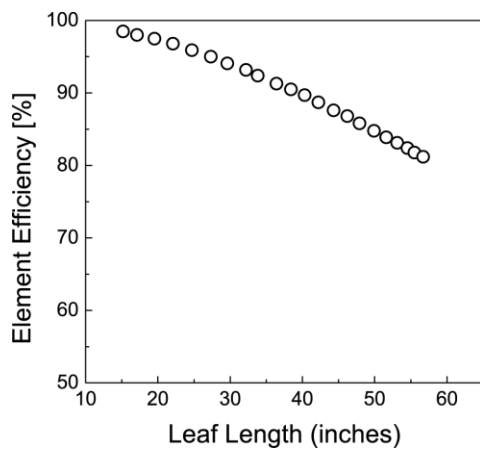


Figure 8: Membrane efficiency decreases monotonically with leaf length due to uneven flux along the length of the leaf. A membrane permeability of $12.3 \text{ L/m}^2\cdot\text{s}\cdot\text{MPa}$ and a friction coefficient of $35 \text{ MPa}\cdot\text{s}/\text{m}^3$ were used in this calculation, and were typical of RO module performance at the time of publication. Modified with permission from Johnson and Busch⁴⁴.

3.2 Pretreatment and salt recovery methods

After concentration by RO, additional treatments may be used to further minimize or eliminate brine discharge, as summarized below.

External reuse: Saline brines with various compositions can be used to irrigate salt-tolerant crops and trees, as water for aquaculture (fish, algae, seaweed, and brine shrimp farming), or stored in solar ponds whose thermal energy can be used to produce heat and electricity; although composition limits and concerns about heavy metal accumulation from brines limit these options³³. A comprehensive list of applications can be found in the Options for Productive Use of Salinity (OPUS) database⁸⁶.

Solar evaporation: Evaporation using shallow (25-45 cm depth) pond is a conventional method for elimination of SWRO brines due to the ease of construction and operation. However, the land areas required can be substantial, (i.e. 13.6-34.3 ha for desalination plants in central Saudi Arabia), limiting this method to areas with high solar flux, low humidity, and low property prices²⁵. Capillaries or wet surfaces can be used to improve evaporation rates, such as in the Wind-Aided Intensified eVaporation (WAIV) process, in which brine is recirculated as a thin falling film to maximize water-air contact and thus maximize evaporation²⁵. Lab-scale tests suggest that this process can reduce the required land area by an order of magnitude²⁵.

Thermal processes: A multi-stage flash or other thermal process can be used, although such methods require a great deal of energy and expense^{28, 34}. For example, when a thermal process was used to remove the remaining 10% of the water from landfill leachates after RO treatment, the thermal process accounted for 35-38% of the overall costs²⁸.

Zero Liquid Discharge (ZLD) salt recovery processes: ZLD processes use a series of concentration and precipitation steps to recover pure water and valuable salts from saline brines, realizing zero waste disposal²⁵. For example, the SAL-PROC method uses a series of steps: concentration by RO or solar evaporation, crystallization using a cooling vessel or crystallizer pond, and precipitation using a reaction vessel with added lime or soda ash³³⁻³⁴. This process produces separate gypsum, calcium carbonate, magnesium hydroxide, sodium chloride, and sodium sulfate products³³⁻³⁴. The ROSP process uses evaporative crystallization to produce NaCl and evaporative cooling to produce Na₂SO₄³⁴. Revenue from salt products could cover about 2/3 of the separation cost for brackish water purification, although the economics would change for HPRO due to changes in feed composition and applied pressure. We note that NaCl is commercially produced from seawater, and Mg(OH)₂ has been in the past²⁰. This suggests the potential economic benefits of recovering byproducts from brine to compensate for some of the cost of desalination.

Bipolar Membrane Electrodialysis (BMED): BMED provides an alternative method for recovering useful chemical from RO brines – acids and bases rather than salts. An electrical potential gradient drives the preferential diffusion of anions and cations through selective membranes, and into compartments in which they combine with hydrogen and hydroxide ions respectively. These H⁺ and OH⁻ ions are generated from the disassociation of water at bipolar membranes. The acids and bases (primarily NaOH and HCl) can be recovered at concentrations up to 0.2 M³⁶.

Chlor-Alkali Process: Similarly to BMED, this process uses an electrochemical cell to oxidize chloride ions to chlorine gas and convert sodium ions and water to sodium hydroxide^{20, 87}. Hydrogen gas is produced at the cathode, and can be either collected as a commodity, used on site, or directly released to the atmosphere⁸⁷. A membrane cell process outcompetes other configurations such as the diaphragm cell process and the mercury cell process because it produces high-purity NaOH and avoids the environmental problems stemming from heavy metal use⁸⁷.

Electrochlorination (EC): Electrochlorination is a redox process that uses an electrolytic cell to convert NaCl and water to sodium hypochlorite and hydrogen. Although this process and BMED have only been tested at the laboratory scale, a preliminary economic analysis shows that BMED has lower capital and operating costs (\$0.79/m³) than evaporation ponds or ZLD (\$2.04 and \$1.30/m³ respectively). This analysis also showed that although EC had higher costs than the other three processes (\$2.35/m³), sale of hypochlorite could result in a net profit of \$0.85/m³, whereas the other processes would operate at a loss³⁶.

Because this economic analysis was conducted for a brackish water feed, we have redone the calculation of potential revenues for recovered salts and chemicals for SWRO brine, formation water, produced water, and FGD water. **Table 4** shows the amount of salts and other chemicals that could be recovered from each feed, as well as their sale value at current prices of \$42/ton for NaCl, \$60/ton for Cl₂, \$100/ton for Na₂SO₄, \$350/ton for NaOH, \$400/ton for NaOCl, \$200/wet ton (35% acid) for HCl, \$300/ton for H₂SO₄, \$1500/ton for HBr, \$350/ton for HNO₃, and about \$1000/ton for KOH. This analysis shows the most potential revenue from BMED. Given that this process had lower capital and operating costs than the others when brackish water was used as a feed³⁶, BMED will probably be the best option for chemical recovery from the concentrates studied. However, further pilot-scale study of capital and operating costs for acid, base, and salt recovery, as well as an analysis of the price-demand curve for the salts and chemicals produced, would be required to confirm this.

Table 4: Revenues from salt or chemical recovery after concentration using the SAL-PROC, BMED, chlor-alkali, and EC methods. These costs don't include the capital and operating expenses for the recovery, revenues from CaCO₃ and Mg(OH)₂ precipitated during pretreatment, or the effect of salt production from RO on worldwide salt and chemical prices.

	SWRO brine (50% recovery)	Fracking flowback water	Formation water	FGD water
Major ions after pretreatment [symbol, mg/L]	Cl ⁻ (20,000), Na ⁺ (11,000), K ⁺ (400)	Na ⁺ (13,000), Cl ⁻ (12,000), Br ⁻ (300), K ⁺ (300)	Cl ⁻ , Na ⁺ (~10,000 each), Br ⁻ , SO ₄ ²⁻ , NO ₃ ⁻ , K ⁺ (100-1000 each)	Cl ⁻ (1000-28,000), SO ₄ ²⁻ (1500-8000), Na ⁺ (700-5000)
Salts produced by SAL-PROC [symbol, mg/L]	NaCl (28,000)	NaCl (19,700)	NaCl (16,800)	Na ₂ SO ₄ (2100-11,800) + NaCl (900-8100)
Acids and bases produced by BMED [symbol, mg/L]	HCl (20,500), NaOH (19,200), KOH (560)	NaOH (22,800), HCl (12,200), HBr (300), KOH (450)	NaOH (17,200), HCl (10,400), HBr (100-1000), H ₂ SO ₄ (100-1000), HNO ₃ (100-1000), KOH (120-1200)	HCl (1100-28,800), H ₂ SO ₄ (1500-8100), NaOH (1200-8800)
Chemicals produced by the chlor-alkali process [symbol, mg/L]	NaOH (19,200), Cl ₂ (20,000)	NaOH (22,800), Cl ₂ (12,000)	NaOH (17,200), Cl ₂ (10,000)	NaOH (1200-8800), Cl ₂ (1000-28,000)
Amount of hypochlorite from EC [mg/L]	35,500	25,200	21,500	2200 to 16,300
Revenue from SAL-PROC [\$ / m ³ feed]	1.2	0.83	0.71	0.25-1.52

Revenue from BMED [\$/m³ feed]	19.0	15.9	12.9-15.9	1.5-22.0
Revenue from the chlor-alkali process [\$/m³ feed]	7.9	8.7	7.2	0.48-4.76
Revenue from EC [\$/m³ feed]	14.2	10.1	8.6	0.88-6.52

3.3 Recovery of trace metals

Recovering trace metals from seawater has been proposed due to the vast amounts of these species present in sea water compared to those on land⁸⁸, and as a way to defray the costs of brine disposal²⁰. High salinity brine is likely to contain more concentrated metals compared to seawater, allowing a more efficient recovery. Lithium is a minor component in most brines, which can be recovered by proposed processes including adsorption, bioaccumulation, ion-exchange, and membrane processes²⁰. Lithium recovery from seawater is not cost effective compared to extraction from salt beds and ores, and can also be more environmentally destructive than mining²⁰. However, these salt beds and ores are available in only a few countries, and full-scale SWRO facilities to extract Lithium are under construction in Japan and Korea²⁰. Uranium is present in seawater at even lower concentrations (about 3 ppb). A half-wave rectified alternating current electrochemical method (HW-ACE) has been proposed to extract uranium more efficiently than existing physicochemical adsorption methods⁸⁸. This method uses an amidoxime-functionalized electrode surface to adsorb UO_2^+ (along with other cations) and selectively reduce it to UO_2 before releasing the non-reduced cations⁸⁸. Uranium concentrations up to 1.9 g/g can be deposited on the electrode over a 10-20 hour period, although the adsorbed concentration increases with the solution concentration⁸⁸; thus RO brines are a better uranium source for this process than seawater. This method could potentially be applied to the recovery of other trace metals, although different chelating agents and a modified electrical cycle would be needed.

4. Future work and implications

High-pressure reverse osmosis (2500-5000 psi) would allow for the concentration of high-salinity waste streams including SWRO brines, formation waters associated with carbon sequestration, fracking flowback water, and flue gas desulfurization wastewater. The feeds generated from these applications contain a variety of minerals, with typical osmotic pressure ranging widely from ~100 to ~3000 psi. The process provides a potentially more energy-efficient brine concentration method than thermal processes, but a number of challenges remain to be addressed. The divalent cations in these brines are potential scalants that can be removed by the lime and soda ash softening processes commonly used for municipal water treatment. Biofouling will likely present another important challenge to separation, as multiple bacteria species known to cause biofouling grow at the pressures of interest. This problem can be mitigated by strategies such as incorporation of biocidal silver particles into the membrane and feed spacer, advanced feed spacer design, and membrane cleaning, although no method is known to eliminate it. Concentration polarization will require a higher applied pressure especially at high recoveries, but

a slight increase in NaCl diffusivity at increased concentrations will reduce this problem to a certain degree (at salt concentration < 320 g/L).

Disc-tube modules are commonly operated at 1800-3000 psi, while spiral-wound modules have a pressure limit of about 1200 psi. Currently available literature provides little information on the failure mechanisms for spiral-wound modules. The materials and design of the disc-tube modules can serve as a good reference for the improvement of spiral-wound designs. The efficiency of spiral-wound modules can also be improved by increasing the module diameter and number of membrane leaves, and by minimizing the feed-side pressure drop. The high applied pressure still require the module to have a thicker pressure vessel, although the cost of this vessel could be offset because larger RO modules require less piping and fewer RO trains . Finally, because RO cannot reduce the retentate fraction to zero regardless of the applied pressure, a brine disposal method will be necessary. Possible processes for ZLD include salt recovery, the chlor-alkali process, solar evaporation, BMED, and electrochlorination, which all eliminate the liquid waste and recovering salts or other chemicals as valuable byproducts. The BMED process appears to provide the highest high revenue because it converts the salts present into acids and bases with higher value. Overall, HPRO holds promise as a method for disposing of brines from several energy and water-related processes, and improvements in high-pressure module design would be a good first step, as it would allow a more detailed investigation of the module mechanical requirements and RO facility operational and capital costs

Acknowledgment

This material is based on work supported by the Department of Energy under Award Number DE-FE0026308.

Disclaimer

This report was prepared as an account of work sponsored by an agency of the United States Government. Neither the United States Government nor any agency thereof, nor any of their employees, makes any warranty, express or implied, or assumes any legal liability or responsibility for the accuracy, completeness, or usefulness of any information, apparatus, product, or process disclosed, or represents that its use would not infringe privately owned rights. Reference herein to any specific commercial product, process, or service by trade name, trademark, manufacturer, or otherwise does not necessarily constitute its endorsement, recommendation, or favoring by the United States Government or any agency thereof. The views and opinions of authors expressed herein do not necessarily state or reflect those of the United States Government or any agency.

REFERENCES

1. Jiménez, S.; Micó, M.; Arnaldos, M.; Medina, F.; Contreras, S., State of the art of produced water treatment. *Chemosphere* **2018**, *192*, 186-208.
2. Dadari, S.; Rahimi, M.; Zinadini, S., Crude oil desalter effluent treatment using high flux synthetic nanocomposite NF membrane-optimization by response surface methodology. *Desalination* **2016**, *377*, 34-46.
3. Ellis, C. E., Wet air oxidation of refinery spent caustic. *Environ. Prog.* **1998**, *17* (1), 28-30.
4. Tarutis Jr, W. J.; Stark, L. R.; Williams, F. M., Sizing and performance estimation of coal mine drainage wetlands. *Ecol. Eng.* **1999**, *12* (3-4), 353-372.
5. Higgins, T. E.; Sandy, A. T.; Givens, S. W., Flue gas desulfurization wastewater treatment primer. *Power (New York)* **2009**, *153* (3).
6. Wilkinson, J.; Watt, D.; Headquarters, N., Review of demilitarisation and disposal techniques for munitions and related materials. *MSIAC/NATO/PfP Editor, Report L-118* **2006**.
7. Shi, X.; Lefebvre, O.; Ng, K. K.; Ng, H. Y., Sequential anaerobic-aerobic treatment of pharmaceutical wastewater with high salinity. *Bioresour. Technol.* **2014**, *153*, 79-86.
8. Liu, Y.; Ma, L.; Liu, Y.; Kong, G., Investigation of novel incineration technology for hospital waste. *Environmental science & technology* **2006**, *40* (20), 6411-6417.
9. Chatzisyneon, E.; Xekoukoulotakis, N. P.; Diamadopoulou, E.; Katsaounis, A.; Mantzavinos, D., Boron-doped diamond anodic treatment of olive mill wastewaters: statistical analysis, kinetic modeling and biodegradability. *Water Res.* **2009**, *43* (16), 3999-4009.
10. Zhang, H.; Fang, S.; Ye, C.; Wang, M.; Cheng, H.; Wen, H.; Meng, X., Treatment of waste filtrate oil/water emulsion by combined demulsification and reverse osmosis. *Sep. Purif. Technol.* **2008**, *63* (2), 264-268.
11. Durai, G.; Rajasimman, M., Biological Treatment of Tannery Wastewater- A Review. *Journal of Environmental science and Technology* **2011**, *4* (1), 1-17.
12. Källqvist, T.; Carlberg, G.; Kringstad, A., Ecotoxicological characterization of industrial wastewater—sulfite pulp mill with bleaching. *Ecotoxicol. Environ. Saf.* **1989**, *18* (3), 321-336.
13. Zhou, M.; Tan, Q.; Wang, Q.; Jiao, Y.; Oturan, N.; Oturan, M. A., Degradation of organics in reverse osmosis concentrate by electro-Fenton process. *J. Hazard. Mater.* **2012**, *215*, 287-293.
14. Zhou, M.; Liu, L.; Jiao, Y.; Wang, Q.; Tan, Q., Treatment of high-salinity reverse osmosis concentrate by electrochemical oxidation on BDD and DSA electrodes. *Desalination* **2011**, *277* (1-3), 201-206.
15. Drioli, E.; Curcio, E.; Criscuoli, A.; Di Profio, G., Integrated system for recovery of CaCO₃, NaCl and MgSO₄·7H₂O from nanofiltration retentate. *J. Membr. Sci.* **2004**, *239* (1), 27-38.
16. Ivanovic, I.; Leiknes, T.; Ødegaard, H., Influence of loading rates on production and characteristics of retentate from a biofilm membrane bioreactor (BF-MBR). *Desalination* **2006**, *199* (1), 490-492.
17. Chiang, L.-C.; Chang, J.-E.; Wen, T.-C., Indirect oxidation effect in electrochemical oxidation treatment of landfill leachate. *Water Res.* **1995**, *29* (2), 671-678.
18. Renou, S.; Givaudan, J.; Poulain, S.; Dirassouyan, F.; Moulin, P., Landfill leachate treatment: review and opportunity. *J. Hazard. Mater.* **2008**, *150* (3), 468-493.
19. Kim, D. H., A review of desalting process techniques and economic analysis of the recovery of salts from retentates. *Desalination* **2011**, *270* (1-3), 1-8.

20. Shahmansouri, A.; Min, J.; Jin, L.; Bellona, C., Feasibility of extracting valuable minerals from desalination concentrate: a comprehensive literature review. *Journal of Cleaner Production* **2015**, *100*, 4-16.
21. Fakhru'l-Razi, A.; Pendashteh, A.; Abdullah, L. C.; Biak, D. R. A.; Madaeni, S. S.; Abidin, Z. Z., Review of technologies for oil and gas produced water treatment. *J. Hazard. Mater.* **2009**, *170* (2-3), 530-551.
22. Joo, S. H.; Tansel, B., Novel technologies for reverse osmosis concentrate treatment: A review. *J. Environ. Manage.* **2015**, *150*, 322-335.
23. Dickson, A. G.; Goyet, C., *Handbook of methods for the analysis of the various parameters of the carbon dioxide system in sea water*. publisher not identified: 1994.
24. Madalyn Blondes, K. G., Elisabeth Rowan, James Thordsen, Mark Reidy, Mark Engle, Yousif Kharaka, Burt Thomas, U.S. Geological Survey National Produced Waters Geochemical Database version 2.2. **2016**.
25. Pérez-González, A.; Urtiaga, A.; Ibáñez, R.; Ortiz, I., State of the art and review on the treatment technologies of water reverse osmosis concentrates. *Water Res.* **2012**, *46* (2), 267-283.
26. Duxbury, A.; Byrne, R. H.; Mackenzie, F. T., Chemical and physical properties of seawater. In *Encyclopedia Britannica*, 1998 ed.; 2017.
27. Heijman, S.; Guo, H.; Li, S.; Van Dijk, J.; Wessels, L., Zero liquid discharge: Heading for 99% recovery in nanofiltration and reverse osmosis. *Desalination* **2009**, *236* (1), 357-362.
28. Rautenbach, R.; Linn, T., High-pressure reverse osmosis and nanofiltration, a "zero discharge" process combination for the treatment of waste water with severe fouling/scaling potential. *Desalination* **1996**, *105* (1), 63-70.
29. Baker, R., *Membrane Technology and Applications*. 2nd ed.; Wiley: West Sussex, 2008.
30. Elimelech, M.; Phillip, W. A., The future of seawater desalination: energy, technology, and the environment. *science* **2011**, *333* (6043), 712-717.
31. Shaffer, D. L.; Arias Chavez, L. H.; Ben-Sasson, M.; Romero-Vargas Castrillón, S.; Yip, N. Y.; Elimelech, M., Desalination and reuse of high-salinity shale gas produced water: drivers, technologies, and future directions. *Environmental science & technology* **2013**, *47* (17), 9569-9583.
32. Harto, C.; Veil, J. *Management of water extracted from carbon sequestration projects*; Argonne National Laboratory (ANL): 2011.
33. Ahmed, M.; Arakel, A.; Hoey, D.; Thumarukudy, M. R.; Goosen, M. F.; Al-Haddabi, M.; Al-Belushi, A., Feasibility of salt production from inland RO desalination plant reject brine: a case study. *Desalination* **2003**, *158* (1-3), 109-117.
34. Neilly, A.; Jegatheesan, V.; Shu, L., Evaluating the potential for zero discharge from reverse osmosis desalination using integrated processes—A review. *Desalination and water treatment* **2009**, *11* (1-3), 58-65.
35. Tong, T.; Elimelech, M., The global rise of zero liquid discharge for wastewater management: drivers, technologies, and future directions. *Environmental science & technology* **2016**, *50* (13), 6846-6855.
36. Badruzzaman, M.; Oppenheimer, J.; Adham, S.; Kumar, M., Innovative beneficial reuse of reverse osmosis concentrate using bipolar membrane electro dialysis and electrochlorination processes. *J. Membr. Sci.* **2009**, *326* (2), 392-399.
37. Gingerich, D. B.; Sun, X.; Behrer, A. P.; Azevedo, I. L.; Mauter, M. S., Spatially resolved air-water emissions tradeoffs improve regulatory impact analyses for electricity generation. *Proc. Natl. Acad. Sci.* **2017**, *114* (8), 1862-1867.
38. Al-Karaghoul, A.; Kazmerski, L. L., Energy consumption and water production cost of conventional and renewable-energy-powered desalination processes. *Renewable and Sustainable Energy Reviews* **2013**, *24*, 343-356.

39. Arena, J. T.; Jain, J. C.; Lopano, C. L.; Hakala, J. A.; Bartholomew, T. V.; Mauter, M. S.; Siefert, N. S., Management and dewatering of brines extracted from geologic carbon storage sites. *International Journal of Greenhouse Gas Control* **2017**, *63*, 194-214.
40. Hamed, O.; Zamamiri, A.; Aly, S.; Lior, N., Thermal performance and exergy analysis of a thermal vapor compression desalination system. *Energy Convers. Manage.* **1996**, *37* (4), 379-387.
41. Shaffer, D. L.; Werber, J. R.; Jaramillo, H.; Lin, S.; Elimelech, M., Forward osmosis: where are we now? *Desalination* **2015**, *356*, 271-284.
42. McGinnis, R. L.; Hancock, N. T.; Nowosielski-Slepowron, M. S.; McGurgan, G. D., Pilot demonstration of the NH₃/CO₂ forward osmosis desalination process on high salinity brines. *Desalination* **2013**, *312*, 67-74.
43. McGovern, R. K., On the potential of forward osmosis to energetically outperform reverse osmosis desalination. *J. Membr. Sci.* **2014**, *469*, 245-250.
44. Johnson, J.; Busch, M., Engineering aspects of reverse osmosis module design. *Desalination and Water Treatment* **2010**, *15* (1-3), 236-248.
45. Miyawaki, O.; Saito, A.; Matsuo, T.; Nakamura, K., Activity and activity coefficient of water in aqueous solutions and their relationships with solution structure parameters. *Biosci., Biotechnol., Biochem.* **1997**, *61* (3), 466-469.
46. Chang, Y.; Myerson, A., The diffusivity of potassium chloride and sodium chloride in concentrated, saturated, and supersaturated aqueous solutions. *AIChE J.* **1985**, *31* (6), 890-894.
47. Peters, T. A., Purification of landfill leachate with reverse osmosis and nanofiltration. *Desalination* **1998**, *119* (1), 289-293.
48. Chengda, H. Membrane Pressure Vessels Department. <http://www.chengda-winder.com/en/showproducts.asp?id=5>.
49. Corporation, P. Pall Disc Tube Module System. <https://shop.pall.com/us/en/oil-gas/midstream/midstream-process-water-/pall-disc-tube-module-system-zidgri78l7k>.
50. Sablani, S.; Goosen, M.; Al-Belushi, R.; Wilf, M., Concentration polarization in ultrafiltration and reverse osmosis: a critical review. *Desalination* **2001**, *141* (3), 269-289.
51. *Water Treatment Principles and Design*. 2 ed.; John Wiley and Sons: Hoboken, 2005.
52. Kim, S.; Hoek, E. M., Modeling concentration polarization in reverse osmosis processes. *Desalination* **2005**, *186* (1-3), 111-128.
53. Tan, C. H.; Ng, H. Y., Modified models to predict flux behavior in forward osmosis in consideration of external and internal concentration polarizations. *J. Membr. Sci.* **2008**, *324* (1), 209-219.
54. Wilson, A. D.; Stewart, F. F., Deriving osmotic pressures of draw solutes used in osmotically driven membrane processes. *J. Membr. Sci.* **2013**, *431*, 205-211.
55. Lime and Soda Ash Softening.
56. Feng, D.; Aldrich, C.; Tan, H., Treatment of acid mine water by use of heavy metal precipitation and ion exchange. *Miner. Eng.* **2000**, *13* (6), 623-642.
57. Den, W.; Wang, C.-J., Removal of silica from brackish water by electrocoagulation pretreatment to prevent fouling of reverse osmosis membranes. *Sep. Purif. Technol.* **2008**, *59* (3), 318-325.
58. Sheikholeslami, R.; Bright, J., Silica and metals removal by pretreatment to prevent fouling of reverse osmosis membranes. *Desalination* **2002**, *143* (3), 255-267.
59. Talbot, D., Megascale Desalination. *TECHNOLOGY REVIEW* **2015**, *118* (2), 48-49.
60. Karagiannis, I. C.; Soldatos, P. G., Water desalination cost literature: review and assessment. *Desalination* **2008**, *223* (1-3), 448-456.
61. Duraisamy, R. T.; Beni, A. H.; Henni, A., *State of the art treatment of produced water*. INTECH Open Access Publisher: 2013.
62. Herzberg, M.; Elimelech, M., Biofouling of reverse osmosis membranes: role of biofilm-enhanced osmotic pressure. *J. Membr. Sci.* **2007**, *295* (1), 11-20.

63. Vrouwenvelder, J.; Von Der Schulenburg, D. G.; Kruithof, J.; Johns, M.; Van Loosdrecht, M., Biofouling of spiral-wound nanofiltration and reverse osmosis membranes: a feed spacer problem. *Water Res.* **2009**, *43* (3), 583-594.
64. Cheftel, J. C., Review: High-pressure, microbial inactivation and food preservation. *Revista de Agaroquimica y Tecnologia de Alimentos* **1995**, *1* (2-3), 75-90.
65. ZoBell, C. E.; Johnson, F. H., The influence of hydrostatic pressure on the growth and viability of terrestrial and marine bacteria. *J. Bacteriol.* **1949**, *57* (2), 179.
66. Mitchell, A. C.; Phillips, A. J.; Hiebert, R.; Gerlach, R.; Spangler, L. H.; Cunningham, A. B., Biofilm enhanced geologic sequestration of supercritical CO₂. *International Journal of Greenhouse Gas Control* **2009**, *3* (1), 90-99.
67. Kappachery, S.; Paul, D.; Yoon, J.; Kweon, J. H., Vanillin, a potential agent to prevent biofouling of reverse osmosis membrane. *Biofouling* **2010**, *26* (6), 667-672.
68. Yang, H.-L.; Chun-Te Lin, J.; Huang, C., Application of nanosilver surface modification to RO membrane and spacer for mitigating biofouling in seawater desalination. *Water Res.* **2009**, *43* (15), 3777-3786.
69. Bradford, W. L.; Herrington, R. E.; Clement, A. D., Filtration membrane and method of making same. Google Patents: 2007.
70. Günther, R.; Perschall, B.; Reese, D.; Hapke, J., Engineering for high pressure reverse osmosis. *J. Membr. Sci.* **1996**, *121* (1), 95-107.
71. ROTREAT Radial Channel Disc Tube Module Sizes. <http://rcdt-module.com/> (accessed January 19 2017).
72. Technology, R. S. M. Disc Tube RO Membrane Module for Landfill Leachate. <http://www.risingsunmembranes.com/wastewater-treatment-membranes/disc-tube-ro-nf-membrane/disc-tube-ro-dtro-membrane-module-for.html> (accessed January 19 2017).
73. Grosse, D.; LaMonica, D. *Site Technology Capsule: Rochem Separation Systems, INC., Disc Tube Module Technology*; Cincinatti, Ohio, 1998.
74. Bartels, C.; Hirose, M.; Fujioka, H., Performance advancement in the spiral wound RO/NF element design. *Desalination* **2008**, *221* (1-3), 207-214.
75. Buecker, B., Reverse Osmosis Pre-Treatment: Techniques and Technology. *Engineering* **360** **2016**.
76. Peterson, R.; Greenberg, A.; Bond, L.; Krantz, W., Use of ultrasonic TDR for real-time noninvasive measurement of compressive strain during membrane compaction. *Desalination* **1998**, *116* (2-3), 115-122.
77. Ochoa, N.; Masuelli, M.; Marchese, J., Effect of hydrophilicity on fouling of an emulsified oil wastewater with PVDF/PMMA membranes. *J. Membr. Sci.* **2003**, *226* (1), 203-211.
78. Persson, K. M.; Gekas, V.; Trägårdh, G., Study of membrane compaction and its influence on ultrafiltration water permeability. *J. Membr. Sci.* **1995**, *100* (2), 155-162.
79. Pendergast, M. T. M.; Nygaard, J. M.; Ghosh, A. K.; Hoek, E. M., Using nanocomposite materials technology to understand and control reverse osmosis membrane compaction. *Desalination* **2010**, *261* (3), 255-263.
80. Hussain, Y. A.; Al-Saleh, M. H., A viscoelastic-based model for TFC membranes flux reduction during compaction. *Desalination* **2014**, *344*, 362-370.
81. Pendergast, M. M.; Ghosh, A. K.; Hoek, E., Separation performance and interfacial properties of nanocomposite reverse osmosis membranes. *Desalination* **2013**, *308*, 180-185.
82. Baum, B.; Margosiak, S.; Holley Jr, W., Reverse osmosis membranes with improved compaction resistance. *Industrial & Engineering Chemistry Product Research and Development* **1972**, *11* (2), 195-199.
83. Germain, Y., Burst pressure prediction of polyamide pipes. *Polymer Engineering & Science* **1998**, *38* (4), 657-661.

84. Lee, J.-H.; Chung, J. Y.; Chan, E. P.; Stafford, C. M., Correlating chlorine-induced changes in mechanical properties to performance in polyamide-based thin film composite membranes. *J. Membr. Sci.* **2013**, *433*, 72-79.
85. Maskan, F.; Wiley, D. E.; Johnston, L. P.; Clements, D. J., Optimal design of reverse osmosis module networks. *AIChE J.* **2000**, *46* (5), 946-954.
86. Program, N. D. S. Options for the Productive Use of Salinity.
http://s3.amazonaws.com/zanran_storage/australian-aquacultureportal.com/ContentPages/48337214.pdf.
87. Khursheed, A. F.; Mansfield, C. A.; Depro, B. M.; Perry, V. A., The Chlorine Industry: A Profile. **2000**.
88. Liu, C.; Hsu, P.-C.; Xie, J.; Zhao, J.; Wu, T.; Wang, H.; Liu, W.; Zhang, J.; Chu, S.; Cui, Y., A half-wave rectified alternating current electrochemical method for uranium extraction from seawater. *Nature Energy* **2017**, *2*, 17007.